

Liquid-crystal composites of carbon nanotubes in a magnetic field: Bridging continuum theory and a molecular-statistical approach

Danil A. Petrov ^{*}*Physics of Phase Transitions Department, Perm State University, Bukirev Street 15, 614990 Perm, Russia*

(Received 14 March 2023; accepted 6 May 2023; published 17 May 2023)

We propose an approach combining the continuum theory and molecular-statistical approach for a suspension of carbon nanotubes based on a negative diamagnetic anisotropy liquid crystal. Using the continuum theory, we show that in the case of an infinite sample in suspension it is possible to observe peculiar magnetic Fréedericksz-like transitions between three nematic phases: planar, angular, and homeotropic with different mutual orientations of liquid-crystal and nanotube directors. The transition fields between these phases are found analytically as functions of material parameters of the continuum theory. To account for the effects associated with temperature changes, we propose a molecular-statistical approach that allows obtaining the equations of orientational state for the orientation angles of the main axes of the nematic order, i.e., the liquid-crystal and carbon-nanotube directors in a similar form as was obtained within the continuum theory. Thus, it is possible to relate the parameters of the continuum theory, such as the surface-energy density of a coupling between molecules and nanotubes, to the parameters of the molecular-statistical model and the order parameters of the liquid crystal and carbon nanotubes. This approach allows determining the temperature dependencies of the threshold fields of transitions between different nematic phases, which is impossible in the framework of the continuum theory. In the framework of the molecular-statistical approach we predict the existence of an additional direct transition between the planar and homeotropic nematic phases of the suspension, which cannot be described based on the continuum theory. As the main results, the magneto-orientational response of the liquid-crystal composite is studied and a possible biaxial orientational ordering of the nanotubes in the magnetic field is shown.

DOI: [10.1103/PhysRevE.107.054701](https://doi.org/10.1103/PhysRevE.107.054701)

I. INTRODUCTION

In the physics of liquid crystals (LCs) and composites materials based on them, the continuum theory [1] has proven to be very useful and fruitful. Due to its relative simplicity, this theory allows one to describe quite well the available nematic state and experimentally observed magneto-orientational phenomena, such as Fréedericksz transitions [2–8]. Though, a significant disadvantage of the continuum theory is that it is not suitable for solving problems related to the description of temperature dependencies of the orientational states of the LC matrix and the ensemble of impurity particles. However, the molecular-statistical approach allows one to take into account the temperature dependencies of the orientational states of the system components for LC and composites based on them, and, in particular, the degree of ordering of both the long axes of molecules and anisometric impurity particles in terms of order parameters. The previously proposed statistical mean-field models of LC suspensions of ferroelectric [9,10], magnetic particles [11–13] and carbon nanotubes (CNTs) [14] considered planar coupling of particles to the matrix in the absence of an external field or in a field directed along the polarization or magnetization vector, which, of course, responds to uniaxial ordering. The existing theoretical works do not

cover suspensions with a homeotropic type of orientational coupling of particles with the matrix [15–19] and the possibility of a more general biaxial ordering [16,20–25], arising in an external field during the competition of orientational mechanisms (crossed electric and magnetic fields or different signs of dielectric and diamagnetic anisotropy). One of the goals of this work is to develop a molecular-statistical theory of the mean field for the case of the biaxial nature of the orientational ordering of LC composites of CNTs in a magnetic field. According to the works [26–30], the LC molecules have a planar type of coupling with the CNT surface, due to which in infinite samples in the absence of external fields and bounding planes, the directions of the main axes of the nematic order of the LC molecules and CNTs, i.e., the directors, coincide and are degenerate in orientations. In the case of positive anisotropies of the diamagnetic susceptibility of LC and CNTs, an external magnetic field orients the main axes of the molecules and nanotubes in its direction and thus removes orientation degeneracy. As the field increases, the orientation of the LC and CNT directors does not change, but the degree of ordering of the subsystems grows [14], and the composite itself remains uniaxial. However, if we consider opposite sign anisotropies of diamagnetic susceptibility (competing orientational mechanisms), namely, negative for LC and positive for CNT, we should expect peculiar Fréedericksz-like magnetic transitions, i.e., the mutual orientation of the LC and CNT directors will change in a threshold manner with an increasing

^{*}Corresponding author: petrovda@bk.ru

magnetic field, as was experimentally found for LC composites of CNTs based on nematics with negative anisotropy of dielectric permittivity in the electric field [31,32]. In the first part of the paper we consider the continuum theory for suspension of CNTs in nematic LC with negative anisotropy of diamagnetic susceptibility. Based on the thermodynamic potential—the free energy, whose minimization by the orientation angles of the LC and CNT directors will make it possible to obtain a system of equations of orientational equilibrium. As a result of the analysis and solution of this system, we determine different nematic orientational phases of the composite, which differ in the orientation of the LC and CNT directors relative to the field, and find the threshold magnetic fields of transitions between these phases. In the second part of the paper we consider a tensor version of the molecular-statistical mean-field theory in which each of the macroscopic orientation tensors (LC matrix and CNT ensemble) is characterized by two scalar order parameters, so with this approach the system of orientational equilibrium equations obtained by minimizing the free energy contains two equilibrium equations for orientation angles of the LC and CNT directors as in the continuum theory and four additional integral self-consistency equations for the order parameters. The presented molecular-statistical theory allows considering both the effect of temperature on the orientational structure of LCs and impurity CNTs, through order parameters, and orientational transitions induced by an external magnetic field, through the orientation angles of the LC medium and impurity nanotubes. Thus, another goal of the work is to build a bridge between the continuum theory and the molecular-statistical approach, which makes it possible to determine the temperature dependencies of continuum theory parameters, such as the surface-energy density of a coupling between LC molecules and CNTs, as well as the magnetic fields of peculiar Fréedericksz-like transitions between different nematic orientational phases.

II. CONTINUUM THEORY

A. Free-energy density

In this section, we consider the continuum theory of peculiar Fréedericksz-like magnetic transitions in an infinite and homogeneous CNT suspension in a nematic LC with negative anisotropy of the diamagnetic susceptibility. The theory is based on the previously proposed approach [33–36], where magnetic Fréedericksz transitions were considered for the LC suspension of CNTs in the classical splay geometry. In the case of a boundless sample, we can omit the contributions to the free-energy density of elastic deformations of the LC director and the effects of segregation of impurity particles; then, taking into account the soft planar coupling of the LC molecules to the CNT surface and the diamagnetic properties of the suspension components, we write down according to Ref. [33]

$$F_c = -\frac{1}{2}y_n\mu_0\chi_a^n(\mathbf{nH})^2 - \frac{1}{2}y_p\mu_0\chi_a^p(\mathbf{mH})^2 - y_ny_p\frac{W}{d_p}(\mathbf{nm})^2. \quad (1)$$

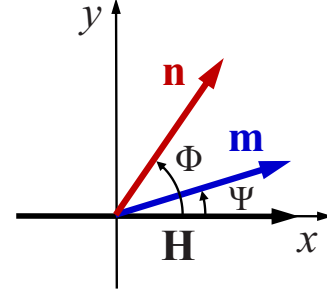


FIG. 1. Geometry.

Here, \mathbf{n} and \mathbf{m} are the unit vectors, known as directors, that represent the main axes of nematic order of the LC molecules and CNTs, respectively; \mathbf{H} is the external magnetic field strength; y_p and $y_n = 1 - y_p$ are volume fractions of the CNT and the LC, respectively; χ_a^n and χ_a^p are the anisotropies of the diamagnetic susceptibility of the LC and the CNT, respectively; μ_0 is the magnetic permeability of the vacuum; W is the surface-energy density of the coupling between the CNTs and the LC molecules; d_p is the transverse diameter of the CNT.

The first two terms in Eq. (1) take into account the diamagnetic properties of the LC matrix and the impurity CNTs, respectively, while the last term is responsible for the finite (soft) coupling of the LC and CNT directors. It should be noted that continuum theories of LC composites of nanoparticles [37–40] usually assume $y_n = 1$ due to the low concentration of impurity, but this assumption will not be used here, for the convenience of comparison with the results of molecular-statistical theory [14,41].

Section II B discusses the derivation of equations describing the equilibrium orientational states of an LC suspension of CNTs in a magnetic field.

B. Orientational equilibrium equations

In the presence of the magnetic field $\mathbf{H} = (H, 0, 0)$ LC molecules tend to rotate orthogonally to the field due to the negative anisotropy of diamagnetic susceptibility, while the CNTs rotate parallel to it (competing orientational mechanisms); then the director components \mathbf{n} and \mathbf{m} can be represented as

$$\mathbf{n} = [\cos \Phi, \sin \Phi, 0], \quad \mathbf{m} = [\cos \Psi, \sin \Psi, 0] \quad (2)$$

(see Fig. 1).

By substituting Eq. (2) into Eq. (1) we obtain

$$F_c(\Phi, \Psi) = \frac{1}{2}y_n\mu_0|\chi_a^n|H^2\cos^2\Phi - \frac{1}{2}y_p\mu_0\chi_a^pH^2\cos^2\Psi - y_ny_p\frac{W}{d_p}\cos^2(\Phi - \Psi). \quad (3)$$

Minimization of the free-energy density (3) by Φ and Ψ allows obtaining the suspension orientational equilibrium equations

$$\frac{1}{2}\mu_0|\chi_a^n|H^2\sin 2\Phi - y_p\frac{W}{d_p}\sin 2(\Phi - \Psi) = 0, \quad (4)$$

$$\frac{1}{2}\mu_0\chi_a^pH^2\sin 2\Psi - y_n\frac{W}{d_p}\sin 2(\Phi - \Psi) = 0. \quad (5)$$

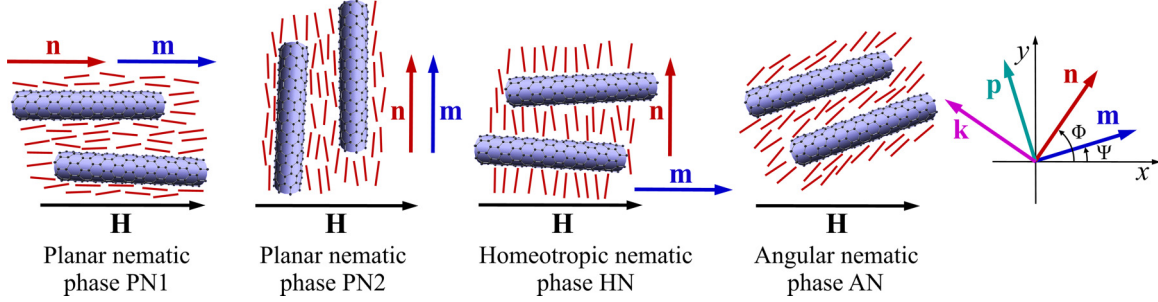


FIG. 2. Orientational phases of the LC composite of CNTs.

This system of equations has four different solutions obeying a minimum of the free-energy density (3)

$$\frac{\partial^2 F_c}{\partial \Phi^2} \geq 0, \quad \frac{\partial^2 F_c}{\partial \Psi^2} \geq 0, \quad \frac{\partial^2 F_c}{\partial \Phi^2} \frac{\partial^2 F_c}{\partial \Psi^2} - \left(\frac{\partial^2 F_c}{\partial \Phi \partial \Psi} \right)^2 \geq 0. \quad (6)$$

All these solutions can be matched with different homogeneous orientational phases. Let us consider these phases in more detail.

C. Orientational phases

The first two solutions of the system of Eqs. (4) and (5) correspond to the values of $\Phi = 0$, $\Psi = 0$ and $\Phi = \pi/2$, $\Psi = \pi/2$, corresponding to the planar coupling of the LC and CNT directors ($\mathbf{n} \parallel \mathbf{m}$). According to Refs. [33,34,39] let us relate these solutions to the first planar nematic phase (PN1) and the second planar nematic phase (PN2), respectively. The PN1 phase corresponds to the orientational structure when the orientations of the directors \mathbf{n} and \mathbf{m} coincide with the direction of the magnetic field \mathbf{H} , and in the phase PN2 the vectors \mathbf{n} and \mathbf{m} are directed orthogonally to the field \mathbf{H} (see Fig. 2). The third solution $\Phi = \pi/2$, $\Psi = 0$ corresponds to the case when the LC director \mathbf{n} is oriented orthogonally to the field \mathbf{H} , and the CNT director \mathbf{m} is parallel to the field \mathbf{H} . This orientational structure corresponds to the homeotropic coupling of the vectors \mathbf{n} and \mathbf{m} ($\mathbf{n} \perp \mathbf{m}$), and its corresponding phase can be called homeotropic nematic (HN) according to Refs. [33,34,39,40]. The latter solution corresponds to the angular nematic phase (AN), in which the orientation angles of the LC and CNT directors can take values from 0 to $\pi/2$ depending on the magnitude of the magnetic field \mathbf{H} and the material parameters of the system [33,34,39,40].

Let us substitute the solutions for the orientation angles of the LC and CNT directors, corresponding to the planar phases PN1 and PN2 and the homeotropic phase HN, into the expression for the free-energy density (1). As a result, we obtain the following, respectively,

$$F_c^{(PN1)} = \frac{1}{2} y_n \mu_0 |\chi_a^n| H^2 - \frac{1}{2} y_p \mu_0 \chi_a^p H^2 - y_n y_p \frac{W}{d_p}, \quad (7)$$

$$F_c^{(PN2)} = -y_n y_p \frac{W}{d_p}, \quad (8)$$

$$F_c^{(HN)} = -\frac{1}{2} y_p \mu_0 \chi_a^p H^2. \quad (9)$$

Comparison of these expressions shows that in the absence of magnetic field $H = 0$ the free-energy densities of the planar phases PN1 and PN2 coincide and do not exceed the value corresponding to the homeotropic phase HN. In the presence of a magnetic field the values of the free-energy densities (7) and (8) differ by the value

$$F_c^{(PN1)} - F_c^{(PN2)} = \frac{1}{2} y_n \mu_0 |\chi_a^n| H^2 (1 - b), \quad b = \frac{y_p \chi_a^p}{y_n |\chi_a^n|}. \quad (10)$$

From this expression, it follows that when $b > 1$, the PN1 phase is stable, and when $b < 1$, the PN2 phase is. Thus, the continuum theory predicts two different sequences of transitions between the orientational phases described above, which have a threshold character and can occur only when the magnetic field reaches a certain critical value. The former is PN1–AN–HN, and the latter is PN2–AN–HN. The final phase is always the homeotropic phase HN, the intermediate phase is the angular phase AN, and the initial phase can be either planar phases PN1 or PN2.

To conclude this section, it is necessary to discuss the symmetry of the above-mentioned nematic orientational phases. As can be seen in Fig. 2 both planar phases PN1 and PN2 correspond to $D_{\infty h}$ point group symmetry. The homeotropic phase HN has the lower D_{2h} symmetry and the angular phase AN has the lowest C_{2h} symmetry with one mirror plane and the C_2 axis normal to it. The symmetry of the angular phase AN is easily determined from the equations of orientational equilibrium (4) and (5) and the components of the LC and CNT directors (2). It can be seen from Eqs. (4) and (5) that adding the value of π to Φ and Ψ does not change the form of the equations, and thus the z axis of the laboratory coordinate system coincides with the C_2 axis (see Fig. 1). The possible biaxial character of the orientational ordering of an LC composite of CNTs induced by a magnetic field will be considered below within the framework of the molecular-statistical theory. The symmetry of LCs, including the biaxial character of the orientational order, is discussed in detail in Refs. [42–46], and in the case of LC colloids, for example, in Refs. [24,47–49].

Note here that for a boundless sample the above-described transitions are a kind of analog of the Fréedericksz magnetic transitions [1,39], since there are some characteristic threshold fields, when reached, the reorientation of the LC and CNT directors occurs. Let us proceed to finding these threshold fields.

D. Orientational transition fields

Let us first find the transition field $H_{\parallel}^{(1)}$ between the PN1 and AN phases. Near $H_{\parallel}^{(1)}$ the deviations of the LC and CNT directors from the magnetic field direction are small $\Phi \ll 1$, $\Psi \ll 1$, so the system of Eqs. (4) and (5) can be linearized and the existence condition for its solution gives

$$H_{\parallel}^{(1)} = \sqrt{a(b-1)}, \quad a = \frac{2y_n W}{\mu_0 \chi_a^p d_p}, \quad (11)$$

where b is defined in Eq. (10).

The transition field $H_{\parallel}^{(2)}$ between the PN2 and AN phases can be determined in a similar way. Near $H_{\parallel}^{(2)}$ the angles Φ and Ψ are close to $\pi/2$, i.e., $\Phi = \pi/2 - \delta\Phi$ and $\Psi = \pi/2 - \delta\Psi$, where $\delta\Phi \ll 1$, $\delta\Psi \ll 1$. In this case, the system of Eqs. (4) and (5) can be represented as a power series expansion in the small values $\delta\Phi$ and $\delta\Psi$. Limiting ourselves to the first order smallness and using the condition that the solution of the system of Eqs. (4) and (5) exists, we obtain

$$H_{\parallel}^{(2)} = \sqrt{a(1-b)}. \quad (12)$$

We can see from the expressions (11) and (12) that they have real values at $b > 1$ and $b < 1$, respectively.

Let us find the last transition field H_{\perp} from the angular phase AN to the homeotropic phase HN. Close to this transition, the CNT director \mathbf{m} is slightly deviated from the orientation of the field \mathbf{H} , while the LC director \mathbf{n} is almost orthogonal to the field, i.e., $\Psi \ll 1$ and $\Phi = \pi/2 - \delta\Phi$, where $\delta\Phi \ll 1$. Expanding Eqs. (4) and (5) in a power series by small Ψ and $\delta\Phi$, using the above procedure, we obtain

$$H_{\perp} = \sqrt{a(1+b)}. \quad (13)$$

From the found expressions (11), (12), and (13) it can be seen that they unambiguously set the values of the fields of transitions between different orientational phases of the suspension for specific values of the volume fraction of impurity y_p , anisotropies of diamagnetic susceptibility of subsystems χ_a^n and χ_a^p , surface-energy density of the coupling between the CNTs and the LC molecules W and transverse diameter of nanotubes d_p . These expressions also show that the field H_{\perp} is always larger than $H_{\parallel}^{(1)}$ and $H_{\parallel}^{(2)}$, which confirms the above-mentioned sequence of transitions between different orientational nematic phases.

E. Conclusions to the continuum theory

The presented continuum theory of magnetically induced orientational phase transitions of LC composites of CNTs is very simple and allows describing the available nematic states of the system in the magnetic field in the case of competing orientational mechanisms. As a result of solving Eqs. (4) and (5), by employing the expressions found for the threshold fields (11), (12), and (13), it is possible to calculate the dependencies of the orientation angles of the LC and CNT directors on the value of the applied magnetic field easily, as, for example, was done for suspensions of magnetic particles in an LC [39]. However, the continuum theory cannot consider the effects associated with changes in temperature. In particular, it is beyond the scope of the theory to study the dependence of the surface density of the coupling energy between the

LC molecules and the CNT W and the threshold transition fields $H_{\parallel}^{(1)}$, $H_{\parallel}^{(2)}$, and H_{\perp} on temperature. Besides, the physical properties of the suspension in a magnetic field and in its absence should be different since the presence of the field leads to the appearance of additional orientational ordering of both LC molecules and CNTs. The molecular-statistical theory, which will be discussed in the next section, can give a simultaneous account of the influence of temperature and magnetic field on the orientational states of the suspension.

III. MOLECULAR-STATISTICAL THEORY

A. Free-energy density

Let us use the previously proposed tensor version of the molecular-statistical theory of LC composites of CNTs [14,41]. In this approach, in addition to the intermolecular-attraction in the LC medium, we take into account the dispersive attraction and steric repulsion of nanotubes, the dispersive attraction between suspension components, as well as the magnetic properties of the LC matrix and the anomalously high diamagnetism of CNTs [50–54]. The effect of the impurity volume fraction, temperature, coupling energy of suspension components, and magnetic field on the orientational ordering of the LC matrix and CNTs was previously studied. The concentration and temperature phase transitions in the suspension for different values of the magnetic field strength have been examined, but only in the case of the uniaxial nature of the orientational ordering. The cases of both positive [14], and negative [41] anisotropy of the diamagnetic susceptibility of the LC matrix have been considered. In the latter case, the magnetic-field induced transitions of an LC from the “easy-axis” state to the “easy-plane” state, which are uniaxial, were considered; thus, the possibility of changing the mutual orientation of the main axes of the LC and CNT nematic order has not been taken into account. The concentration and field shifts of the phase transition point between nematic and isotropic or paranematic phases have also been studied.

The advantage of the previously proposed tensor expression of the free-energy density [14] is that, depending on the phase symmetry, the macroscopic orientation tensors of LC and CNT can be written in either uniaxial or biaxial form. According to Ref. [14], the expression for the free-energy density in the mean-field approximation reads as

$$\begin{aligned} \mathcal{F}_{\text{ms}} &= F_{\text{ms}} \frac{v_n}{\lambda V} \\ &= -\frac{1}{2} y_n^2 \eta_{ik}^n \eta_{ik}^n - \frac{1}{2} y_p^2 \gamma^2 (\omega_p + \kappa \tau) \eta_{ik}^p \eta_{ik}^p - y_n y_p \gamma \omega \eta_{ik}^n \eta_{ik}^p \\ &\quad - \frac{1}{2} \sqrt{\frac{2}{3}} h_i h_k (-y_n \eta_{ik}^n + y_p \gamma \xi \eta_{ik}^p) + y_n \tau \langle \ln \mathcal{W}_n \rangle \\ &\quad + y_p \gamma \tau \langle \ln \mathcal{W}_p \rangle. \end{aligned} \quad (14)$$

Here, v_n is the volume of the LC molecule, $v_p = \pi d_p^2 l_p / 4$ is the volume of the cylindrical CNT, d_p and l_p are the transverse diameter and the length of the CNT, respectively, V is the suspension volume. We also introduce the value $\lambda = A_n / v_n$, which is the Meier-Saupe mean-field constant [55], which corresponds to the interaction energy A_n of the LC molecules. The interaction of the suspension components is determined

by the dimensionless parameter $\omega = A/A_n$, where A is the energy of orientational interaction between the nanotubes and the LC molecules. The parameter $\omega_p = A_p/A_n$ describes the relative role of the energy of interaction A_p between impurity CNTs. Below we will consider the case of positive ω , then in the absence of a magnetic field the preferred orientation of the long axes of the nematic molecules and the CNTs will coincide, corresponding to the planar coupling of the LC and CNT directors. According to Ref. [9], the parameter ω is proportional to the coupling energy of the particles with the LC matrix and the form factor of the particles. The latter is zero if the particles have a spherical shape, i.e., ω is also a measure of the anisotropy of the particles: more elongated CNTs correspond to larger values of this parameter. The parameter $\kappa = 5l_p/(4\gamma d_p)$ accounts for the excluded CNT volume in the second virial approximation for cylindrical particles, i.e., the steric repulsion of CNTs [56–59]. In Eq. (14) we also introduce dimensionless temperature $\tau = k_B T/\lambda$ (k_B is the Boltzmann constant, T is absolute temperature), magnetic field strength $h = H\sqrt{\mu_0}|\tilde{\chi}_a^n|/\lambda$ and the parameter $\gamma = v_n/v_p$, responsible for the relative sizes of the LC molecule and CNT. The parameter $\xi = \tilde{\chi}_a^p/|\tilde{\chi}_a^n|$ is responsible for the relative contribution of diamagnetic orientational mechanisms associated with the CNTs and the LC, where $\tilde{\chi}_a^n < 0$ and $\tilde{\chi}_a^p > 0$ are the anisotropies of the diamagnetic susceptibility of single LC molecule and single CNT, respectively. The higher the value ξ , the greater the contribution of the CNTs to the magneto-orientational response of the composite. Angle brackets in Eq. (14) denote the statistical averaging over the single-particle distribution functions \mathcal{W}_n and \mathcal{W}_p , respectively, of the LC molecules and CNTs according to the orientations of their long axes.

The free-energy density (14) includes tensors of the orientation η_{ik}^n and η_{ik}^p of the LC and CNT subsystems, respectively. They are discussed in more detail in the next section.

B. Order parameters

In previous papers [14,41], the cases when the main axes of the nematic order, the LC and CNT directorices, were fixed in space are considered. As shown in the preceding section, in a magnetic field, due to the opposite sign of the diamagnetic susceptibility anisotropies of the subsystems, the nematic and nanotube directors can change their orientation, so the expressions for the orientation tensors η_{ik}^n and η_{ik}^p should be presented in the biaxial form [60,61]

$$\eta_{ik}^n = \sqrt{\frac{3}{2}}R_n \left(l_i l_k - \frac{1}{3}\delta_{ik} \right) + \frac{Q_n}{\sqrt{2}}(n_i n_k - k_i k_k), \quad (15)$$

$$\eta_{ik}^p = \sqrt{\frac{3}{2}}R_p \left(l_i l_k - \frac{1}{3}\delta_{ik} \right) + \frac{Q_p}{\sqrt{2}}(m_i m_k - p_i p_k), \quad (16)$$

through the triplets of unit orthogonal vectors

$$\begin{aligned} \mathbf{n} &= [\cos \Phi, \sin \Phi, 0], \quad \mathbf{l} = [0, 0, 1], \quad \mathbf{k} = \mathbf{l} \times \mathbf{n}, \\ \mathbf{m} &= [\cos \Psi, \sin \Psi, 0], \quad \mathbf{p} = \mathbf{l} \times \mathbf{m}, \end{aligned} \quad (17)$$

where the components of the vectors \mathbf{n} and \mathbf{m} remain the same as in the continuum theory [see Eq. (2) and Fig. 2]. The arbitrary factors of $\sqrt{3/2}$ and $1/\sqrt{2}$ multiplying the first and second terms for both tensors (15) and (16), respectively,

have been inserted for later convenience (see Appendix A). Here, we introduce scalar order parameters that depend on the dimensionless temperature τ and the magnetic field h as statistical averages of the Legendre polynomials P_2 :

$$R_n = \langle P_2(\mathbf{l}\mathbf{v}) \rangle, \quad Q_n = \frac{1}{\sqrt{3}} \langle P_2(\mathbf{n}\mathbf{v}) - P_2(\mathbf{k}\mathbf{v}) \rangle, \quad (18)$$

$$R_p = \langle P_2(\mathbf{l}\mathbf{e}) \rangle, \quad Q_p = \frac{1}{\sqrt{3}} \langle P_2(\mathbf{m}\mathbf{e}) - P_2(\mathbf{p}\mathbf{e}) \rangle. \quad (19)$$

Here, \mathbf{v} and \mathbf{e} are unit vectors along the long axis of the LC molecule and CNT, respectively.

Orientation tensors of the LC (15) and the CNT (16) admit three uniaxial structures with the directors \mathbf{l} , \mathbf{n} , \mathbf{k} , and \mathbf{l} , \mathbf{m} , \mathbf{p} , respectively. For $Q_n = 0$, we obtain a uniaxial nematic LC with the director \mathbf{l} , similarly for the ensemble of impurity particles for $Q_p = 0$ we obtain a uniaxial structure with the director \mathbf{l} . At $Q_n = \mp\sqrt{3}R_n$ we obtain for the LC uniaxial structures with the directors \mathbf{n} and \mathbf{k} , respectively, and for the CNT ensemble at $Q_p = \mp\sqrt{3}R_p$, we get uniaxial structures with directors \mathbf{m} and \mathbf{p} , respectively. Thus, the parameters Q_n and Q_p , respectively, characterize the difference in the probability of orientations of LC molecules with respect to the vectors \mathbf{n} and \mathbf{k} , and CNT with respect to the vectors \mathbf{m} and \mathbf{p} . Under the influence of the magnetic field, the main axes of the nematic order \mathbf{n} and \mathbf{m} or the directors of the LC and the CNT (see Fig. 2), can rotate (angular phase) around the vector \mathbf{l} , which is considered constant. In this case, the order parameters Q_n , R_n , Q_p , and R_p are independent variables and for convenience we can introduce an additional system of the order parameters:

$$S_n = \frac{\sqrt{3}Q_n - R_n}{2} = \langle P_2(\mathbf{n}\mathbf{v}) \rangle, \quad (20)$$

$$D_n = \frac{Q_n + \sqrt{3}R_n}{2} = \frac{1}{\sqrt{3}} \langle P_2(\mathbf{l}\mathbf{v}) - P_2(\mathbf{k}\mathbf{v}) \rangle, \quad (20)$$

$$S_p = \frac{\sqrt{3}Q_p - R_p}{2} = \langle P_2(\mathbf{m}\mathbf{e}) \rangle, \quad (21)$$

$$D_p = \frac{Q_p + \sqrt{3}R_p}{2} = \frac{1}{\sqrt{3}} \langle P_2(\mathbf{l}\mathbf{e}) - P_2(\mathbf{p}\mathbf{e}) \rangle. \quad (21)$$

Hereafter, we will mainly consider the positive values of Q_n and Q_p , i.e., when the main axes of the nematic order of the LC and CNT, respectively, are the vectors \mathbf{n} and \mathbf{m} . Consideration of the negative values Q_n and Q_p , at which the vectors \mathbf{k} and \mathbf{p} are the main axes of the nematic order of the LC and the CNT, respectively, is excessive, since the rotation of the vectors \mathbf{n} and \mathbf{m} around the direction \mathbf{l} is determined by the angles Φ and Ψ .

From the definitions (20) and (21), we can see that the parameters S_n and S_p characterize the degree of ordering of the LC molecules and CNTs in the directions \mathbf{n} and \mathbf{m} , respectively, while D_n and D_p serve as a measure of biaxiality. It should be noted here that the biaxial ordering associated with the nonzero order parameter D_n is also specific for the LC molecules themselves if they are chiral (see, for example, Refs. [60,62,63]).

Now we turn to obtaining the equations of the orientational state of the composite, which allow determining the equilibrium values of the order parameters Q_n , R_n , Q_p , and R_p .

C. Equations of orientational state

To determine the equilibrium values of the distribution functions \mathcal{W}_n and \mathcal{W}_p , which, using the self-consistency Eqs. (18) and (19) enable us to find the order parameters

of the composite, we need to solve the variation problem of the minimum (14). Minimization \mathcal{F}_{ms} must be carried out with additional normalization conditions for the distribution functions, which have the form:

$$\int \mathcal{W}_n d\mathbf{v} = 1, \quad \int \mathcal{W}_p d\mathbf{e} = 1. \quad (22)$$

After calculating the convolutions of the tensors (15) and (16) (see Appendix A), the expression for the free-energy density (14) takes the form:

$$\begin{aligned} \mathcal{F}_{ms} = & -\frac{1}{2}y_n^2(Q_n^2 + R_n^2) - \frac{1}{2}y_p^2\gamma^2(\omega_p + \kappa\tau)(Q_p^2 + R_p^2) - y_n y_p \gamma \omega (Q_n Q_p \cos 2(\Phi - \Psi) + R_n R_p) \\ & + \frac{1}{6}h^2[y_n(\sqrt{3}Q_n \cos(2\Phi) - R_n) - y_p \gamma \xi(\sqrt{3}Q_p \cos(2\Psi) - R_p)] + y_n \tau \langle \ln \mathcal{W}_n \rangle + y_p \gamma \tau \langle \ln \mathcal{W}_p \rangle, \end{aligned} \quad (23)$$

to which we need to add terms

$$\Lambda_n \left(\int \mathcal{W}_n d\mathbf{v} - 1 \right) + \Lambda_p \left(\int \mathcal{W}_p d\mathbf{e} - 1 \right), \quad (24)$$

to account for the normalization conditions (22) using the Lagrange multiplier method, where Λ_n and Λ_p are the Lagrange multipliers. The variation of (23) by \mathcal{W}_n and \mathcal{W}_p with regard to the definitions (18) and (19) allows one to obtain the normalized result for single-particle distribution functions of the LC molecules and CNTs over the orientations of their long axes, respectively,

$$\mathcal{W}_n = \frac{\exp \left\{ \frac{2}{3} \varsigma_n [P_2(\mathbf{n}\mathbf{v}) - P_2(\mathbf{k}\mathbf{v})] - \frac{2}{3} \sigma_n P_2(\mathbf{l}\mathbf{v}) \right\}}{\int \exp \left\{ \frac{2}{3} \varsigma_n [P_2(\mathbf{n}\mathbf{v}) - P_2(\mathbf{k}\mathbf{v})] - \frac{2}{3} \sigma_n P_2(\mathbf{l}\mathbf{v}) \right\} d\mathbf{v}}, \quad (25)$$

$$\mathcal{W}_p = \frac{\exp \left\{ \frac{2}{3} \varsigma_p [P_2(\mathbf{m}\mathbf{e}) - P_2(\mathbf{p}\mathbf{e})] - \frac{2}{3} \sigma_p P_2(\mathbf{l}\mathbf{e}) \right\}}{\int \exp \left\{ \frac{2}{3} \varsigma_p [P_2(\mathbf{m}\mathbf{e}) - P_2(\mathbf{p}\mathbf{e})] - \frac{2}{3} \sigma_p P_2(\mathbf{l}\mathbf{e}) \right\} d\mathbf{e}}, \quad (26)$$

where the following notations are introduced:

$$\sigma_n = -\frac{3}{2\tau} \left(y_n R_n + y_p \gamma \omega R_p + \frac{1}{6} h^2 \right), \quad \varsigma_n = \frac{\sqrt{3}}{2\tau} \left(y_n Q_n + y_p \gamma \omega Q_p \cos 2(\Phi - \Psi) - \frac{\sqrt{3}}{6} h^2 \cos 2\Phi \right), \quad (27)$$

$$\sigma_p = -\frac{3}{2\tau} \left(y_n \omega R_n + y_p \gamma (\omega_p + \kappa\tau) R_p - \frac{1}{6} \xi h^2 \right), \quad \varsigma_p = \frac{\sqrt{3}}{2\tau} \left(y_n \omega Q_n \cos 2(\Phi - \Psi) + y_p \gamma (\omega_p + \kappa\tau) Q_p + \frac{\sqrt{3}}{6} \xi h^2 \cos 2\Psi \right). \quad (28)$$

Order parameters R_n , Q_n , R_p , and Q_p can be determined by means of self-consistency conditions (18), (19), and distribution functions (25) and (26) through relations

$$R_n = 1 - \frac{3}{2} \frac{\partial \ln J(\sigma_n, \varsigma_n)}{\partial \sigma_n}, \quad Q_n = \frac{\sqrt{3}}{2} \frac{\partial \ln J(\sigma_n, \varsigma_n)}{\partial \varsigma_n}, \quad (29)$$

$$R_p = 1 - \frac{3}{2} \frac{\partial \ln J(\sigma_p, \varsigma_p)}{\partial \sigma_p}, \quad Q_p = \frac{\sqrt{3}}{2} \frac{\partial \ln J(\sigma_p, \varsigma_p)}{\partial \varsigma_p}, \quad (30)$$

which are the equations of the orientational state of the LC-CNT composite. Here we introduce the notation

$$J(\sigma, \varsigma) = \int_0^1 \exp\{\sigma(1-x^2)\} I_0[\varsigma(1-x^2)] dx, \quad (31)$$

where I_0 is a modified Bessel function of the first kind.

The equations of the orientational state (29) and (30), which allows determining the dependencies of order parameters on temperature and magnetic field strength, should be supplemented with the equations of orientational equilibrium for the orientation angles of the LC and CNT directors Φ and Ψ , respectively. To do this, we substitute the found distribution functions

(25) and (26) in Eq. (23), as a result, the free-energy density takes the form

$$\begin{aligned} \Delta\mathcal{F}_{\text{ms}} = & \frac{1}{2}y_n^2(Q_n^2 + R_n^2 - 2R_n) + \frac{1}{2}y_p^2\gamma^2(\omega_p + \kappa\tau)(Q_p^2 + R_p^2 - 2R_p) + y_n y_p \gamma \omega [Q_n Q_p \cos 2(\Phi - \Psi) + R_n R_p - R_n - R_p] \\ & + \frac{1}{6}h^2(-y_n + y_p \gamma \xi) - y_n \tau \ln J(\sigma_n, \varsigma_n) - y_p \gamma \tau \ln J(\sigma_p, \varsigma_p). \end{aligned} \quad (32)$$

Here, $\Delta\mathcal{F}_{\text{ms}} = \mathcal{F}_{\text{ms}} - \mathcal{F}_{\text{ms}}^{(\text{iso})}$, where $\mathcal{F}_{\text{ms}}^{(\text{iso})}$ is the free-energy density of the isotropic phase, for which R_n, Q_n, R_p, Q_p , and h are equal to zero.

With minimizing Eq. (32) by Φ and Ψ considering Eqs. (18), (19), (29), and (30), we obtain

$$h^2 \sin 2\Phi - 2\sqrt{3}y_p \gamma \omega Q_p \sin 2(\Phi - \Psi) = 0, \quad (33)$$

$$\xi h^2 \sin 2\Psi - 2\sqrt{3}y_n \omega Q_n \sin 2(\Phi - \Psi) = 0. \quad (34)$$

These equations for the orientation angles of the directors \mathbf{n} and \mathbf{m} , obtained on the basis of the molecular-statistical approach, are similar to those obtained in the continuum theory (4) and (5). Thus, the system of Eqs. (29) and (30) together with Eqs. (33) and (34) makes it possible not only to describe the different orientational phases of the LC-CNT composite induced by a magnetic field, but also, unlike the equations of continuum theory (4) and (5) enables us to study the effect of the temperature on the degree of the composite components ordering.

Let us now turn to obtaining expressions for the threshold transition fields between the nematic phases PN1, PN2, HN, and AN, now using the results of the molecular-statistical approach.

D. Orientational transition fields

Equations (33) and (34) describe the same orientational nematic phases: PN1, PN2, HN, and AN as Eqs. (4) and (5). The procedure for finding the threshold fields of transitions between these phases is described in Sec. II D, here we present only the final results.

The transition field from planar phase PN1 to angular phase AN takes the form

$$h_{\parallel}^{(1)} = \sqrt{\tilde{a}(\tilde{b} - 1)}, \quad (35)$$

where

$$\tilde{a} = \frac{2\sqrt{3}y_n \omega Q_n}{\xi}, \quad \tilde{b} = \frac{y_p \gamma Q_p \xi}{y_n Q_n}. \quad (36)$$

The transition fields PN2–AN and AN–HN, respectively, have the form

$$h_{\parallel}^{(2)} = \sqrt{\tilde{a}(1 - \tilde{b})}, \quad (37)$$

$$h_{\perp} = \sqrt{\tilde{a}(1 + \tilde{b})}. \quad (38)$$

Expressions for threshold fields (35), (37), and (38) now implicitly depend not only on the temperature τ through the order parameters Q_n and Q_p , but also on the magnetic field h . Thus, the determination of the transition fields $h_{\parallel}^{(1)}$, $h_{\parallel}^{(2)}$, and h_{\perp} now requires solving the system of Eqs. (29) and (30) together with the condition of equality of the current value of

the field h with one of the field values (35), (37), and (38), as well as the fixed angles Φ and Ψ . So, to find the field $h_{\parallel}^{(1)}$ we need to use conditions $\Phi = \Psi = 0$ and $h_{\parallel}^{(1)} - h = 0$, for the field $h_{\parallel}^{(2)}$ $-\Phi = \Psi = \pi/2$ and $h_{\parallel}^{(2)} - h = 0$, and for the field h_{\perp} $-\Phi = \pi/2$, $\Psi = 0$ and $h_{\perp} - h = 0$.

E. Relationship between the parameters of the continuum theory and the molecular-statistical approach

By comparing the expressions for the free-energy densities (3) and (23), bringing trigonometric functions with angles Φ and Ψ to the same form, considering the definitions of the dimensionless field $h = H\sqrt{\mu_0 \tilde{\chi}_a^n / \lambda}$ and the parameter $\xi = \tilde{\chi}_a^p / |\tilde{\chi}_a^n|$, it is possible to express the parameters of the continuum theory through the parameters of the molecular-statistical approach:

$$\chi_a^n = \frac{2\tilde{\chi}_a^n}{\sqrt{3}v_n} Q_n, \quad \chi_a^p = \frac{2\tilde{\chi}_a^p}{\sqrt{3}v_p} Q_p, \quad \frac{W}{d_p} = \frac{2\lambda\omega}{v_p} Q_n Q_p. \quad (39)$$

It is interesting to note that these values do not depend on the order parameters R_n and R_p . As a result of solving the system of Eqs. (29) and (30) for PN1, PN2, or HN phases, and in the case of the angular phase AN, this system must be supplemented by the Eqs. (33) and (34), it is possible to calculate the dependencies of the order parameters Q_n and Q_p , together with the parameters of the continuum theory χ_a^n , χ_a^p , and W on temperature and external magnetic field.

F. Estimates of material parameters

For further calculations, we introduce estimates of dimensionless values and parameters of the suspension. According to Refs. [14,41] let us assume for the anisotropy of the diamagnetic susceptibility of one LC molecule $|\tilde{\chi}_a^n| \approx |\chi_a^n|v_n \approx 4\pi \times 10^{-7} \text{ nm}^3$. In the framework of the Maier-Saupe theory, the mean-field constant λ is proportional to nematic-isotropic liquid transition temperature T_c^{LC} , $\lambda = 4.55k_B T_c^{\text{LC}}$ [55], which at $T_c^{\text{LC}} \sim 300 \text{ K}$ gives $\lambda \sim 10^{-20} \text{ J}$, then the dimensionless magnetic field $h = H\sqrt{\mu_0 |\tilde{\chi}_a^n| / \lambda}$ becomes of the order of unity at $H \approx 10^9 \text{ A m}^{-1}$. In a previous paper [41] it is shown that the anisotropy of the diamagnetic susceptibility of a single CNT $\tilde{\chi}_a^p$ depends not only on the diameter d_p and the length l_p , but also the number of graphene layers forming it [64]. So, for a separate single-layer CNT with a diameter of $d_p = 2 \text{ nm}$ and the length of $l_p = 100 \text{ nm}$ we get $\tilde{\chi}_a^p \sim 4\pi \times 10^{-3} \text{ nm}^3$, which gives an estimate for the parameter $\xi = \tilde{\chi}_a^p / |\tilde{\chi}_a^n| = 10^4$. As the number of layers increases, the CNT mass increases in proportion to $\tilde{\chi}_a^p$. The method for calculating the CNT mass as well as the anisotropy of the diamagnetic susceptibility is presented in Refs. [41,65]. For CNT with the diameter of $d_p = 2 \text{ nm}$ and the length of $l_p = 100 \text{ nm}$ we obtain $\gamma = v_n / v_p = 1.32 \times 10^{-3}$ and

$\kappa = 5l_p/(4\gamma d_p) = 4.75 \times 10^4$, where according to Ref. [14] it is accepted as follows: $v_n = 0.414 \text{ nm}^3$. It was noted earlier that the ω parameter, which is responsible for the orientational coupling of the LC molecules and CNTs, is related to the form factor of impurity particles and takes large values for strongly anisometric objects, such as CNTs. Based on the estimates presented in Ref. [11], we will assume in further calculations $\omega = 10$. The volume fraction of CNTs in the LC can vary over a wide range $y_p = 10^{-5} - 10^{-2}$ according to Refs. [29,66–69], but for accuracy, we take the value of $y_p = 0.02$. The initial and all subsequent expressions for the free-energy density of molecular-statistical theory (14), (23) and (32) are written in general form and include both dispersive attraction and steric repulsion contributions of CNTs. For low impurity concentrations and for temperatures close to the transition point of a nematic-isotropic liquid ($\tau \approx 0.2$) the CNT attraction can be neglected compared to the steric repulsion, and therefore we can assume $\omega_p = 0$ in numerical calculations.

IV. RESULTS AND DISCUSSION

This section presents the results of numerical solution of equations of orientational state for the LC suspension of CNTs (29), (30), (33), and (34). We have considered various orientational phase diagrams of the composite in a magnetic field and temperature dependencies of threshold fields (35), (37), and (38). Besides we have presented the field dependencies of the orientation angles of the directors and order parameters of the LC and the CNTs, and shown the possibility of the appearance of biaxial nature of the orientational ordering of CNTs in the magnetic field. In the following calculations, we have used the following fixed values of the material parameters: $y_p = 0.02$, $\gamma = 1.32 \times 10^{-3}$, $\kappa = 4.75 \times 10^4$ and $\omega_p = 0$.

A. Temperature dependencies of order parameters

Let us first consider the temperature dependencies of the order parameters of the suspension in the absence of a magnetic field, shown in Fig. 3. The solid lines here correspond to stable solutions, and the dotted lines indicate unstable and metastable solutions. At $h = 0$ and fixed angles $\Phi = 0$ and $\Psi = 0$ the system of orientational state Eqs. (29) and (30) admits three equivalent solutions, which describe uniaxial structures with LC and CNT directors \mathbf{l} , $\mathbf{n} = \mathbf{m}$ and $\mathbf{k} = \mathbf{p}$ [see definition (17) and Fig. 2]. As an example, in Fig. 3 one such solution is presented, where the main axes of the nematic order of the LC and CNT correspond to the vectors \mathbf{n} and \mathbf{m} , respectively, i.e., the first planar phase PN1. In this case the biaxiality parameters D_n and D_p are equal to zero ($Q_n = -\sqrt{3}R_n$ and $Q_p = -\sqrt{3}R_p$) and there remain only two independent order parameters S_n and S_p , determining the degree of ordering of LC molecules and CNTs relative to the same direction $\mathbf{n} = \mathbf{m}$ [see definitions (20) and (21)]. The temperature dependencies S_n and S_p are shown in Fig. 3(a), which demonstrates that as τ increases, the ordering of the long axes of LC molecules and CNTs decreases, and when the temperature reaches the critical value $\tau = \tau_{NI} = 0.21601$ the first-order transition to the isotropic phase I with zero values of the order parameters takes place. The transition

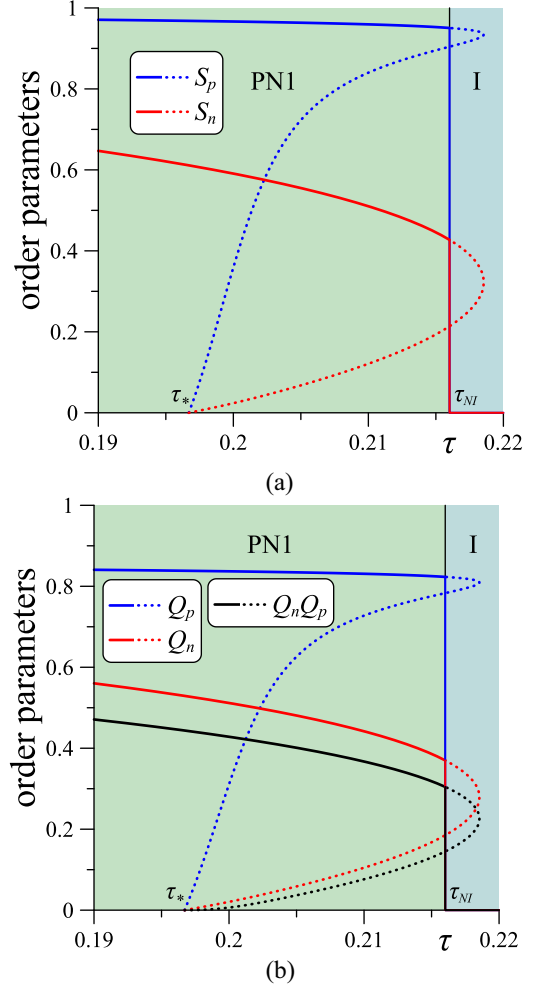


FIG. 3. Temperature dependencies of the LC and CNT order parameters for $\omega = 10$ (a) LC and CNT order parameters responsible for the degree of ordering of molecules and impurity particles relative to the director $\mathbf{n} = \mathbf{m}$ at $\Phi = \Psi = 0$ and (b) order parameters determining the temperature dependencies of continuum theory parameters (39).

temperature τ_{NI} can be determined from the joint solution of the system of orientational state Eqs. (29) and (30) and additional condition of equality of free-energy densities of ordered and isotropic phases $\Delta\mathcal{F}_{ms} = 0$ [see expression (23)]. In Fig. 3 there is another important temperature, namely the point of absolute instability of the isotropic phase relative to the transition to the ordered phase, known as the Curie-Weiss temperature $\tau_* = 0.19670$, for which an analytical expression was previously obtained [14]:

$$\tau_* = \frac{y_n}{10} \left[1 + \sqrt{1 + \frac{20y_p\gamma\omega^2}{(5 - y_p\gamma\kappa)}} \right]. \quad (40)$$

Further, it should be noted that according to Ref. [14] the volume fraction y_p and aspect ratio (l_p/d_p) of CNTs can be chosen so that, due to steric interactions, even in the absence of a magnetic field at high temperatures, nanotubes can be in an ordered phase. Due to the coupling of the LC molecules with the CNTs, the ordering of the latter is transferred to the

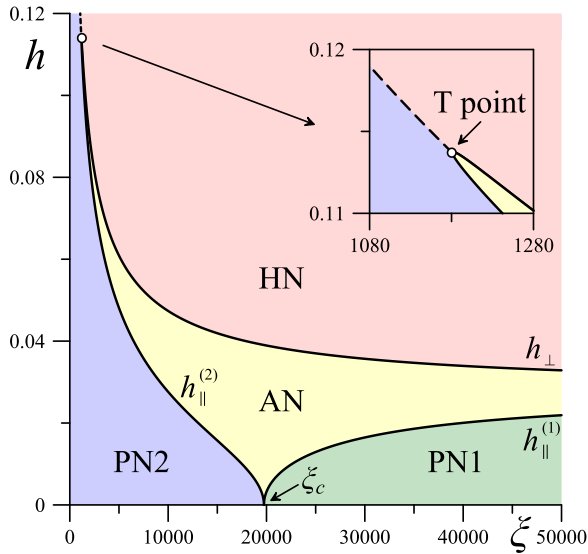


FIG. 4. Orientational phase diagram of the suspension on the magnetic field h -parameter ξ plane for $\tau = 0.21$ and $\omega = 10$.

matrix, and the whole system will be in the weakly ordered paranematic phase P instead of the isotropic state. The influence of the CNT sizes, concentration, and the coupling energy on the phase transitions between the nematic, paranematic, and isotropic phases is discussed in detail in Refs. [14,41].

Figure 3(b) shows temperature dependencies of order parameters Q_n , Q_p and their product $Q_n Q_p$ [see expressions (18) and (19)], which allow one to calculate the temperature dependencies of the parameters of the continuum theory χ_a^n , χ_a^p , and W in accordance with the relations (39). From Fig. 3 we can see that the order parameters of the CNT ensemble S_p and Q_p are weakly dependent on temperature, while the LC subsystem is characterized by a significant decrease in ordering with increasing temperature. This also leads to a significant decrease in the anisotropy of the diamagnetic susceptibility of the LC χ_a^n and the surface coupling energy density of the LC and CNT W (see the red and black curves in Fig. 3(b), respectively). For the temperature $\tau = 0.21$ and coupling energy $\omega = 10$ in the following calculations, using Eq. (39), we obtain $W = 4.7 \times 10^{-4} \text{ J m}^{-2}$, which agrees well with the experimental data [70].

B. Orientational phase diagrams: The influence of the magnetic field

Let us move on to the effects associated with the magnetic field. Figure 4 presents the diagram of orientational nematic phases of an LC suspension of CNTs on the magnetic field h -the parameter ξ plane. Recall that this parameter is responsible for the relative contribution of two diamagnetic orientational mechanisms of magnetic field influence on the structure of the LC-composite. Figure 4 shows, that there is a critical value of the parameter $\xi = \xi_c = 19739.67$, above which, i.e., at $\xi > \xi_c$ with switching the magnetic field on, the planar phase PN1 is stable, and at $\xi < \xi_c$ the planar phase PN2 is. The value ξ_c can be found by jointly solving the system of orientational state Eqs. (29) and (30) with the additional condition of equality of threshold fields $h = h_{\parallel}^{(1)}$ and $h = h_{\parallel}^{(2)}$,

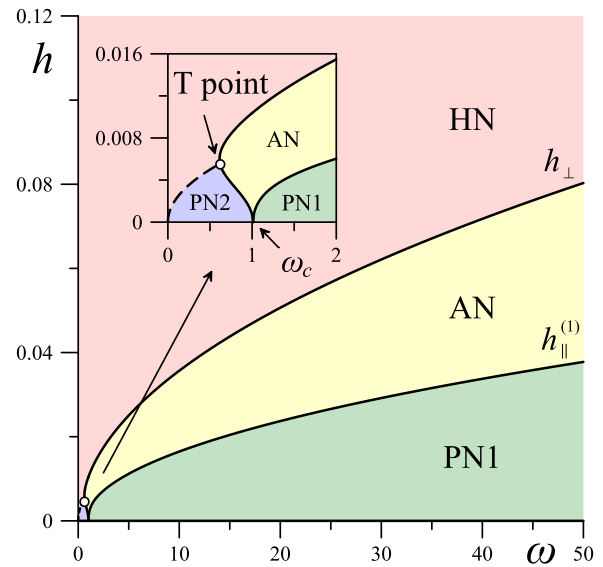


FIG. 5. Orientational phase diagram of the suspension on the magnetic field h -coupling energy ω plane for $\tau = 0.21$ and $\xi = 3 \times 10^4$.

which is reduced to a simple equation $\tilde{b} = 1$ [see expressions (36)]. As the magnetic field increases, both planar phases PN1 and PN2 cease to be stable and a peculiar Fréedericksz-like transition into the angular phase AN occurs at $h = h_{\parallel}^{(1)}$ and $h = h_{\parallel}^{(2)}$, respectively. In large fields exceeding $h = h_{\perp}$, the homeotropic phase HN is stable.

The inset of Fig. 4 shows the part of the diagram containing the triple T point ($\xi = \xi_T = 1181.22$), where the second planar, angular, and homeotropic nematic phases coexist. Figure 4 shows that as ξ approaches ξ_T , the difference of the threshold fields $h_{\perp} - h_{\parallel}^{(2)}$ decreases and turns to zero at the T point. It is found that at $\xi < \xi_T$ as the magnetic field increases, the LC molecules remain oriented predominantly orthogonal to the field $\Phi = \pi/2$ with the main axis of the nematic order \mathbf{n} , while the long CNT axes rotate orthogonally to the field, i.e., $\Psi = \pi/2$ (see Fig. 2). As the magnetic field increases, the nanotube order parameter Q_p decreases and reaches zero value, which is indicated by the dashed line in Fig. 4. For this line order parameter R_p is negative, which corresponds to the orientational anisotropy of the “easy-plane” type, i.e., the long CNT axes are oriented in a plane orthogonal to the vector \mathbf{l} . As the magnetic field grows further, the Q_p parameter becomes negative and increases by absolute value. Thus, in the case of $\xi < \xi_T$ there are no peculiar Fréedericksz-like transitions (angular phase AN is absent), the CNTs are reoriented without rotating the main axis of the nematic order \mathbf{m} -direct transition from the planar phase PN2 to the homeotropic phase HN. Positive values of Q_p correspond to the planar phase PN2, and negative values correspond to the homeotropic phase HN with the main axes of the nematic order of CNTs \mathbf{m} and \mathbf{p} , respectively (see Fig. 2).

Figures 5 and 6 show diagrams of the orientational phases of the suspension on the magnetic field h -coupling energy ω plane for $\xi = 3 \times 10^4$ and $\xi = 10^4$, respectively. Figure 5 shows, that for high coupling energies there is a sequence

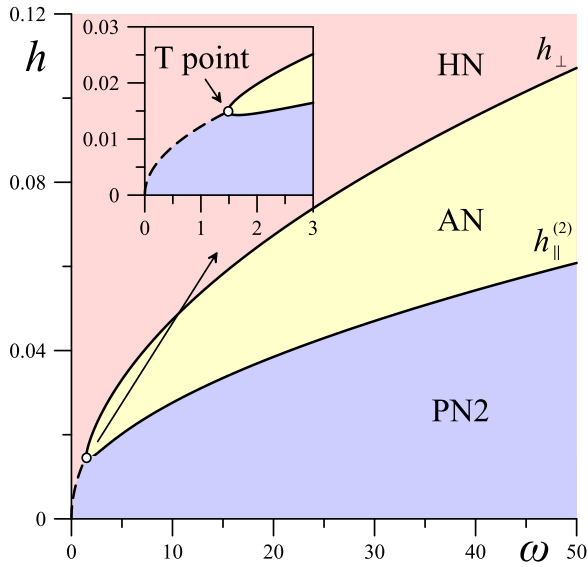


FIG. 6. Orientational phase diagram of the suspension on the magnetic field h -coupling energy ω plane for $\tau = 0.21$ and $\xi = 10^4$.

of PN1-AN-HN transitions. As ω decreases, the first planar phase PN1 becomes unstable and at $\omega_T < \omega < \omega_c$ the transition sequence changes to PN2-AN-HN, where $\omega_c = 1.01$ (see inset in Fig. 5), and the coupling energy $\omega = \omega_T = 0.62$ corresponds to the T point. For $\omega < \omega_T$ as the field increases, there is only a direct transition from the planar phase PN2 to the homeotropic phase HN.

As we can see from Fig. 6 for $\xi = 10^4$ the planar phase PN1 is unstable for any positive ω , but as in the previous case, there is a T point $\omega = \omega_T = 1.48$, to the left of which under the action of the magnetic field there is a direct transition from the planar phase PN2 to the homeotropic phase HN. In Figs. 5 and 6 direct transitions correspond to the dashed lines, for which, as for the phase diagram shown in Fig. 4, the CNT order parameter Q_p turns to zero, i.e., the direct transition changes the sign of Q_p , which corresponds to the reorientation of the CNT in the direction of the field.

Figures 7 and 8 show diagrams of the orientational phases of the suspension on the magnetic field h -temperature τ plane for $\xi = 3 \times 10^4$ and $\xi = 10^4$, respectively. The solid lines correspond to the threshold transition fields between the orientational phases, and the dash-dotted lines correspond to the equilibrium first-order phase transitions from strongly ordered nematic phases PN1, PN2, AN, and HN to the weakly ordered paranematic phase P, which is induced by the magnetic field. In the present paper, the focus is on the orientational phase transitions induced by an external magnetic field and the orientational structure of the composite in the paranematic phase P is not considered.

From the comparison of Figs. 7 and 8 we can see that the transition field $h_{\parallel}^{(1)}$ increases as the temperature rises, and $h_{\parallel}^{(2)}$ decreases, i.e., the magnetic field stabilizes the initial orientational structure of the nematic in the PN1 phase and destabilizes it in the PN2 phase. The transition field from the angular phase AN to the homeotropic phase HN h_{\perp} for both cases decreases with the temperature rise. It is interesting to note here that for $\xi = 3 \times 10^4$ (see Fig. 7) as the magnetic

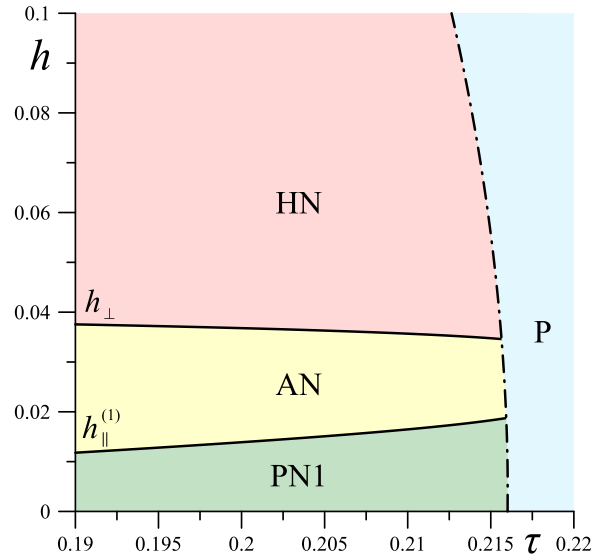


FIG. 7. Orientational phase diagram of the suspension on the magnetic field h -temperature τ plane for $\omega = 10$ and $\xi = 3 \times 10^4$.

field increases, lower temperatures are required for the transition to the paranematic phase P, that is, the magnetic field destabilizes the homeotropic phase, while for $\xi = 10^4$ (see Fig. 8) the opposite effect is observed, namely the magnetic field stabilizes the homeotropic phase HN and as h increases, higher temperatures are required for the transition to the paranematic phase P.

C. Magneto-orientational response of the composite

Figures 9 and 10 show orientational responses of the LC composite of CNTs to an external magnetic field for $\xi = 3 \times 10^4 > \xi_c$ and $\xi = 10^4 < \xi_c$, respectively. In the first case, according to the diagrams shown in Figs. 4 and 5, switching the magnetic field on leads to the preferential orientation of

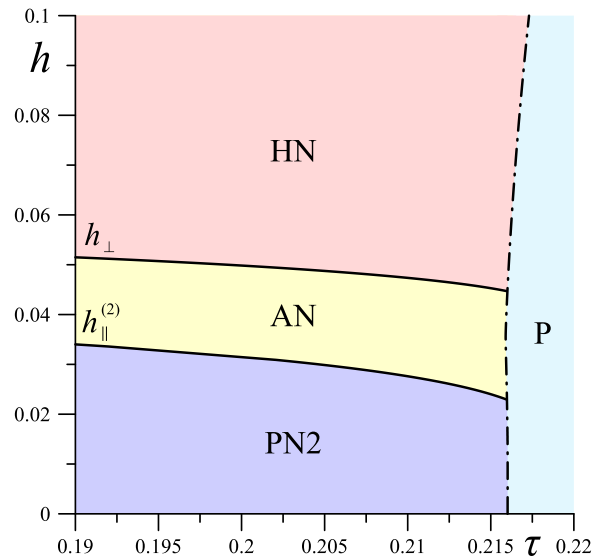


FIG. 8. Orientational phase diagram of the suspension on the magnetic field h -temperature τ plane for $\omega = 10$ and $\xi = 10^4$.

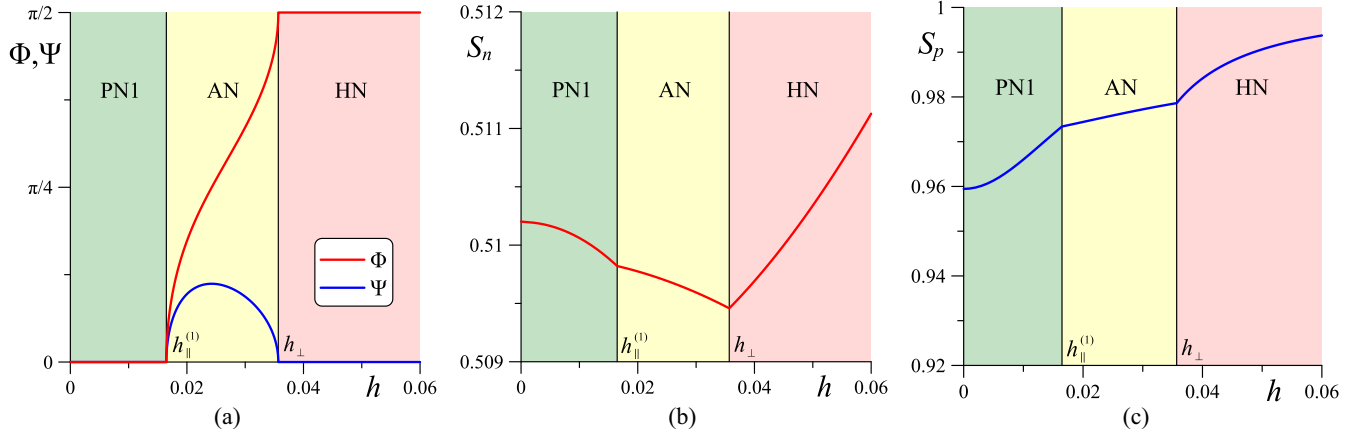


FIG. 9. Orientational response of the suspension to an external magnetic field for $\tau = 0.21$, $\xi = 3 \times 10^4$: (a) orientation angles of the LC and CNT directors, (b) the nematic LC order parameter, which is responsible for the degree of ordering of molecules relative to the director \mathbf{n} , (c) the nematic order parameter of CNTs, which is responsible for the degree of ordering of nanotubes relative to the director \mathbf{m} .

the long axes of the LC molecules and CNTs in the direction of the field \mathbf{H} , i.e., the first planar phase PN1 is stable, for which $\Phi = 0$ and $\Psi = 0$ [see Figs. 2 and 9(a)]. The planar phase PN1 ceases to be stable when the magnetic field reaches the first threshold value $h_{\parallel}^{(1)} = 0.01647$, above which the peculiar Fréedericksz-like transition into the angular phase AN occurs. In this phase, the orientation angles of the LC and CNT directors increase with increasing field, i.e., due to the negative anisotropy of diamagnetic susceptibility, the long axes of the nematic molecules rotate orthogonal to the field direction, entraining the CNTs as a result of orientational coupling between the composite components. With further growth of the magnetic field due to the positive anisotropy of the diamagnetic susceptibility, the nanotubes begin to rotate backward in the direction of the magnetic field, and the angle Ψ upon reaching the maximum value begins to decrease. When the magnetic field reaches the second threshold value $h_{\perp} = 0.03568$ there is a transition to a homeotropic phase HN with fixed values of the orientation angles of the directors of the LC $\Phi = \pi/2$ and the CNTs $\Psi = 0$. Figures 9(b) and 9(c)

show dependencies of the nematic order parameters of the LC S_n and impurity subsystem S_p [see the definitions (20) and (21)], describing the degree of orientational ordering of the long axes of the LC molecules and CNTs, respectively, along the vectors \mathbf{n} and \mathbf{m} . These figures show that the magnetic field disorders the LC molecules and orders the CNTs in the planar phase PN1 and angular phase AN. In the final homeotropic phase HN, both order parameters S_n and S_p increase as the magnetic field grows.

In the second case $\xi = 10^4 < \xi_c$, shown in Fig. 10, according to the diagrams in Figs. 4 and 6 in weak fields, the second planar phase PN2 is stable, in which the long axes of the LC molecules and CNTs are oriented orthogonal to the magnetic field and $\Phi = \Psi = \pi/2$. As can be seen in Fig. 10(a) this phase remains stable until the magnetic field exceeds the threshold value $h_{\parallel}^{(2)} = 0.02761$. Above this value, there is a transition to the angular phase AN, in which, due to the positive anisotropy of the diamagnetic susceptibility, the CNTs begin to rotate in the direction of the magnetic field and transfer this rotation to the matrix. As the magnetic field

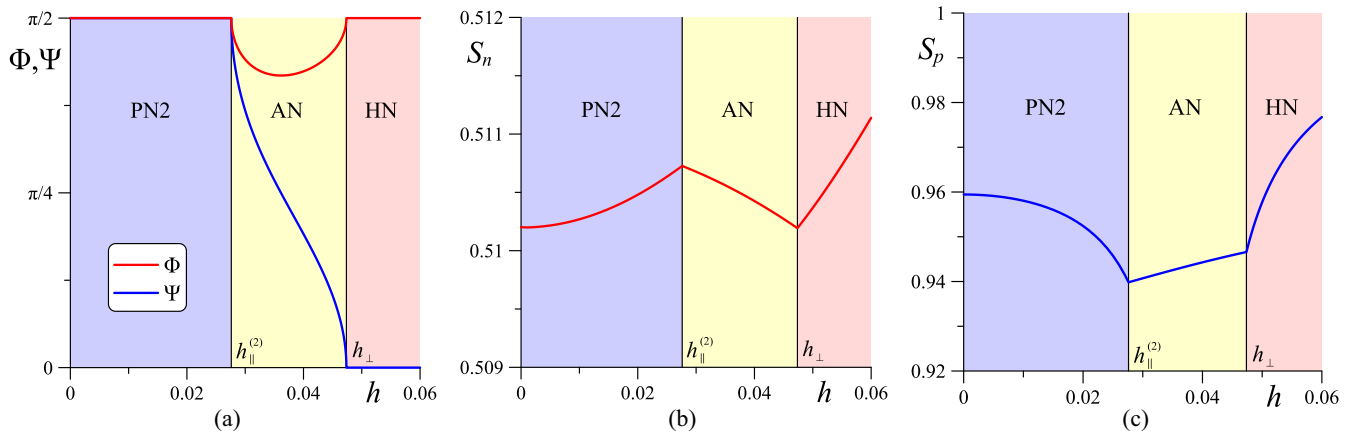


FIG. 10. Orientational response of the suspension to an external magnetic field for $\tau = 0.21$, $\xi = 10^4$: (a) orientation angles of the LC and CNT directors, (b) the nematic LC order parameter, which is responsible for the degree of ordering of the molecules relative to the director \mathbf{n} , (c) the nematic order parameter of CNTs, which is responsible for the degree of ordering of nanotubes relative to the director \mathbf{m} .

increases in the angular phase AN, the orientation angle of the CNT director Ψ decreases gradually and reaches zero value at the second threshold field $h = h_{\perp} = 0.04736$, above which the homeotropic phase HN is stable. In turn, the orientation angle of the LC director Φ in the angular phase AN decreases as the field increases and reaches the minimum, and then increases to $\pi/2$, when the transition to the homeotropic phase HN occurs at $h = h_{\perp}$. In contrast to the previous case ($\xi = 3 \times 10^4$) for $\xi = 10^4$ in the planar phase PN2, the magnetic field orders the LC matrix and disorders the nanotubes, as can be seen from the comparison of Figs. 9(b) and 10(b), as well as Figs. 9(c) and 10(c). These figures show that in the angular phase AN and homeotropic phase HN, the behaviors of the order parameters for $\xi = 3 \times 10^4$ and $\xi = 10^4$ are similar.

Figures 9 and 10 demonstrate that for the presented range of values, the magnetic field insignificantly changes the ordering of the LC molecules and CNTs toward the directors \mathbf{n} and \mathbf{m} , respectively, in all the orientational nematic phases. It should be noted that the calculation results showed that the values of the biaxial parameters D_n and D_p [see definitions (20) and (21)] remain close to zero and do not exceed 0.02 (by absolute value in the case of $D_p < 0$) both for $\xi = 3 \times 10^4$ and $\xi = 10^4$. The parameters Q_n and Q_p , included in Eqs. (33) and (34), which make it possible to determine the equilibrium values of the orientation angles of the LC and CNT directors Φ and Ψ , also exhibit a slight change with an increase in the magnetic field. From this we can conclude that, for the presented values of the material parameters, the continuum theory, which does not take into account the influence of the magnetic field on the material parameters of the system, correctly describes the behavior of the LC composite. However, the situation changes with approaching the T point near which the order parameter Q_p decreases significantly and turns to zero at the T point. Together with that according to Eq. (39) the continuum theory parameters such as the anisotropy of diamagnetic susceptibility of nanotubes χ_a^p and surface-energy density of the coupling between the CNTs and the LC molecules W behave similarly. Thus, near the T point, the results of the continuum theory diverge from the molecular-statistical approach, since the parameters χ_a^p and W cannot be considered independent on the magnetic field. Next, we will consider in detail the behavior of the composite close to the T point.

To conclude this part, we should note that in Figs. 9 and 10 we only present stable solutions corresponding to the minimum values of the free-energy density (23). The analysis of stable and unstable solutions is presented in the Appendix B.

D. Behavior of the composite near the triple point

As noted above, when approaching the triple T point, the difference of the threshold fields $h_{\perp} - h_{\parallel}^{(2)}$ decreases and turns to zero at this point. At the same time the CNT order parameter Q_p also decreases and reaches zero both at the T point and at the point of direct transition between phases PN2 and HN (see the dashed line in Figs. 4–6). At the same time, near the T point, the magnetic field induces biaxial orientational ordering of the disperse subsystem. The degree of biaxiality of the CNT ensemble can be determined using the

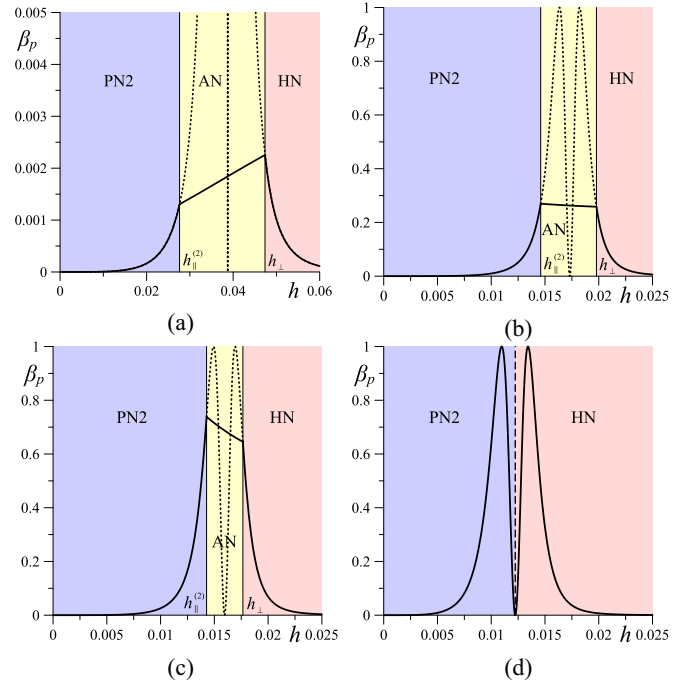


FIG. 11. Dependence of the CNT biaxiality parameter on the magnetic field for $\tau = 0.21$, $\xi = 10^4$ at (a) $\omega = 10$, (b) $\omega = 2$, (c) $\omega = 1.7$, and (d) $\omega = 1$. The triple T point corresponds to $\omega = \omega_T = 1.48$.

parameter [71]

$$\beta_p = 1 - 6 \frac{(\eta_{ik}^p \eta_{kj}^p \eta_{ji}^p)^2}{(\eta_{ik}^p \eta_{ik}^p)^3} = 1 - \frac{R_p^2 (R_p^2 - 3Q_p^2)^2}{(R_p^2 + Q_p^2)^3}. \quad (41)$$

This parameter lies in the range from 0 to 1. In uniaxial phases $\beta_p = 0$, while $\beta_p = 1$ corresponds to maximum biaxiality. Figure 11 shows the dependencies of CNT biaxiality degree on the magnetic field for different values of coupling energy ω distant and close to the T point $\omega = \omega_T = 1.48$. Solid curves correspond to stable solutions and dotted curves to unstable ones. The biaxiality parameter of the LC subsystem β_n , which can be obtained by replacing the index p with n in Eq. (41), remains close to zero for all investigated parameters and is not considered further.

According to the diagram presented in Fig. 6, and Fig. 11(a) away from the T point at $\omega = 10$, the CNT biaxiality parameter increases slightly as the magnetic field approaches the threshold $h_{\parallel}^{(2)}$. As the field increases in the angular phase AN, the biaxiality parameter continues to increase and after the transition to the homeotropic phase HN at $h > h_{\perp}$ decreases in a monotonous manner. The situation is different when approaching the T point, when the difference in the threshold fields decreases $h_{\perp} - h_{\parallel}^{(2)}$. Figures 11(b) and 11(c) show the cases of $\omega = 2$ and $\omega = 1.7$, respectively, which illustrate that the biaxiality parameter increases significantly as the field approaches the threshold value $h_{\parallel}^{(2)}$ of the peculiar Fréedericksz-like transition and reaches its maximum at the transition point. With further growth of the field in the angular phase AN, the biaxiality parameter slightly decreases and after transition to the

homeotropic phase HN continues to decrease. Here it should be noted that the dotted lines in the angular phase AN correspond to unstable solutions of the system of equations of orientational state (29) and (30), which were constructed at fixed values of the orientation angles of the LC and CNT directors both for $\Phi = \Psi = \pi/2$ and $\Phi = \pi/2, \Psi = 0$. From the comparison of Figs. 11(b) and 11(c), it can be seen that the biaxial character of the orientational ordering of CNTs becomes stronger as we approach the T point.

The cases considered before satisfy the condition $\omega > \omega_T$, when the existence of an angular phase AN is possible. In Fig. 11(d) there is a case of $\omega = 1$, when the angular phase AN is absent, because $\omega < \omega_T$. Figure 11(d) shows that previously unstable solutions, which were located in the angular phase AN, become stable, and the biaxiality parameter reaches a maximum value twice as the field increases to the left and right of the point of a direct transition between phases PN2 and HN. At fixed values of macroscopic angles $\Phi = \Psi = \pi/2$ positive values of Q_p correspond to the PN2 phase, and negative values correspond to the homeotropic phase HN. The transition point corresponds to the zero value of both parameters Q_p and β_p . Thus, for CNT suspensions based on a nematic LC with the negative anisotropy of diamagnetic susceptibility, the maximum biaxiality of the impurity subsystem can be detected near the T point. In other words, the biaxial ordering of impurity particles in an LC matrix induced by a magnetic field is possible with weak anchoring of LC molecules with the CNT surface for $\omega \sim 0.1-1$. Based on the values of the material parameters presented above, for such ω we obtain an estimate for the magnetic field $H \sim 10^6-10^7$ A m⁻¹ required to induce the maximum biaxiality of CNTs.

E. Conclusions to the molecular-statistical theory

In contrast to the continuum theory, the presented molecular-statistical approach made it possible to take into account both the influence of the magnetic field and the temperature on the ordering of the LC and CNTs. Equations (33) and (34) for the orientation angles of the LC and CNT directors obtained within the framework of the statistical theory are similar to those found within the continuum theory (4) and (5). Equations (33) and (34) together with the expressions for the transition fields (35), (37), and (38) make it possible to describe the same PN2, PN2, AN, and HN orientational phases as the continuum theory Eqs. (4), (5), (11), (12), and (13). However, several fundamental differences between the two approaches have been found. First of all, as can be seen from the expressions (11), (12), and (13), obtained within the framework of the continuum theory, as the surface-energy density of the coupling between the LC molecules and CNTs decreases, the W values of the threshold fields monotonically decrease and go to zero at $W = 0$, i.e., the angular phase AN exists at any positive W . This result contradicts the phase diagrams presented in Figs. 5 and 6, according to which the angular phase disappears at finite coupling energies of the LC and the CNTs ω . One more result is existence of the direct transition from the planar phase PN2 to the homeotropic phase HN without transition to the intermediate angular phase AN. The next important result of the molecular-statistical approach is the discovery of the triple T point where PN2, AN, and HN

phases coexist. These results can in no way be obtained within the continuum theory. It is shown that, far from the T point, the material parameters of the suspension weakly depend on the magnetic field strength and the results of the continuum theory and molecular-statistical approaches should coincide. Near the T point, the biaxial nature of orientational ordering of CNTs occurs, the nanotube order parameter Q_p decreases considerably with increasing magnetic field, and the material parameters of the suspension, such as the anisotropy of the CNT diamagnetic susceptibility χ_a^p and the surface-energy density of the coupling between the LC and nanotubes W , change along with it [see expressions (39)]. In this case, the results of the continuum theory and the molecular-statistical theory diverge.

V. CONCLUSION

The paper proposes a method of bridging the continuum theory to the molecular-statistical approach to describe a spatially homogeneous CNT suspension in a nematic LC located in the magnetic field. We have considered the case of opposite sign anisotropies of diamagnetic susceptibility of the composite components, which leads to competition of orientational mechanisms in the magnetic field and changes in the mutual orientation of the main axes of the nematic order of the LC and the CNTs.

Within the continuum theory, it has been established that with increasing magnetic field the conditions of the CNT coupling with the LC matrix change in a threshold way: the initial planar type of coupling is consistently transformed through the angular type into the homeotropic one. We have obtained analytical expressions for the threshold fields of peculiar Fréedericksz-like magnetic transitions between nematic orientational phases, which correspond to different types of coupling of the LC molecules and CNTs.

To construct the molecular-statistical theory of CNT suspensions in an LC, we used the previously proposed expression for the free-energy density written in a tensor form [14]. Using the biaxial form of the orientation tensors for the LC and CNTs, we have obtained a system of four integral equations of the orientational state for the scalar order parameters. Through minimizing the free-energy density by the orientation angles of the LC and CNT directors, we have obtained two additional equations similar to those found in the continuum theory. This approach allowed relating the material parameters of the continuum theory, which include the surface-energy density of the coupling between the LC molecules and CNTs as well as the anisotropy of the diamagnetic susceptibility of the dispersion medium and the impurity subsystem, to the order parameters of the molecular-statistical theory. As a result, we have found temperature dependencies of the threshold fields of transitions between different nematic phases that differ in the type of the LC and CNT orientational coupling. We have studied the magneto-orientational response of the composite and constructed the temperature and field dependencies of the LC and impurity subsystems order parameters. It has been found that when the orientational coupling of the LC matrix and the CNTs is weak, with an increase in the magnetic field there can occur a direct transition from the nematic phase with the planar coupling

to the phase with the homeotropic coupling, bypassing the states with angular coupling. This result cannot be reached within the continuum theory. We have studied the biaxial orientational ordering of CNTs in the LC matrix induced by the magnetic field.

The molecular-statistical approach proposed in this work is the most general, since it includes the biaxial form of the orientation tensors of the LC and impurity subsystem. This allows further consideration of LC composites with different types of particles, where there is a competition of orientational mechanisms and the existence of angular orientational coupling between the directors of LC and the impurity particles is possible. Besides, there can be specific nontrivial distributions of director and order parameters in the presence of nanotubes, or nanoparticles, or even flat surfaces (see, for example, Refs. [72–74]), which requires further development of the molecular-statistical theory.

ACKNOWLEDGMENTS

This work was supported by the Foundation for the Advancement of Theoretical Physics and Mathematics “BASIS” and Ministry of Science and Higher Education of the Russian Federation (Project No. FSNF-2023-0004). The author is grateful to Pavel V. Krauzin and anonymous referees for valuable comments.

APPENDIX A: TENSOR CONVOLUTIONS

Normalization of tensors η_{ik}^n and η_{ik}^p [see expressions (15) and (16)] is chosen so that their convolutions have a simple form

$$\begin{aligned}\eta_{ik}^n \eta_{ik}^n &= Q_n^2 + R_n^2, & \eta_{ik}^p \eta_{ik}^p &= Q_p^2 + R_p^2, \\ \eta_{ik}^n \eta_{ik}^p &= Q_n Q_p \cos 2(\Phi - \Psi) + R_n R_p.\end{aligned}\quad (\text{A1})$$

Tensor convolutions η_{ik}^n and η_{ik}^p with the magnetic field vector \mathbf{h} give as follows:

$$\begin{aligned}\sqrt{\frac{2}{3}} h_i h_k \eta_{ik}^n &= \frac{1}{3} h^2 (\sqrt{3} Q_n \cos 2\Phi - R_n), \\ \sqrt{\frac{2}{3}} h_i h_k \eta_{ik}^p &= \frac{1}{3} h^2 (\sqrt{3} Q_p \cos 2\Psi - R_p).\end{aligned}\quad (\text{A2})$$

APPENDIX B: ANALYSIS OF THE FREE-ENERGY DENSITY

Figure 12 shows field dependencies of the free-energy density (32), corresponding to different solutions of the system of Eqs. (29), (30), (33), and (34). The solid lines here correspond to thermodynamically stable solutions selected from the condition of minimum free-energy density (32), and the dotted lines represent the unstable ones. The calculation results in Figs. 12(a) and 12(b) correspond to the magneto-orientational responses of the suspension shown in Figs. 9 and 10, respectively. In Fig. 12 there are no solutions for the isotropic phase at $h = 0$ ($\mathcal{F}_{\text{ms}} = 0$) and the weakly ordered paranematic phase for the studied magnetic field values $h \neq 0$, since they correspond to larger values of the free-energy density.

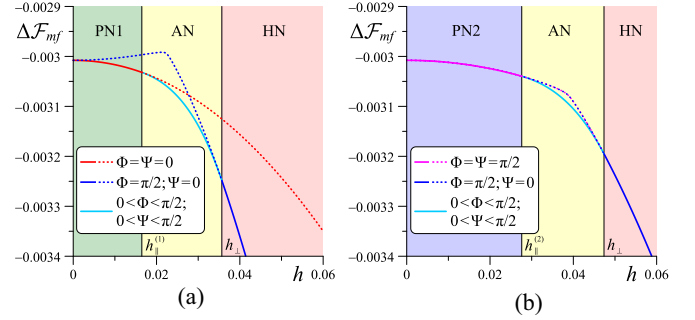


FIG. 12. Dependencies of the free-energy density on the magnetic field for $\omega = 10$, $\tau = 0.21$ at (a) $\xi = 3 \times 10^4$ and (b) $\xi = 10^4$.

Figure 12(a) shows that for $\xi = 3 \times 10^4 > \xi_c$ the first planar phase PN1 is stable until $h < h_{\parallel}^{(1)}$ (the curve $\Phi = \Psi = 0$), at $h_{\parallel}^{(1)} < h < h_{\perp}$ after a peculiar Fréedericksz-like transition, the stable one is the angular phase AN (the curve $0 < \Phi < \pi/2$; $0 < \Psi < \pi/2$), where, as the field increases, the LC director rotates \mathbf{n} in the direction of the field according to Fig. 9(a). In the magnetic fields exceeding $h = h_{\perp}$, stable solutions are those corresponding to the homeotropic phase HN [the curve $\Phi = \pi/2$; $\Psi = 0$ in Fig. 12(a)]. If we neglected the existence of the angular phase AN, i.e., we neglect the possibility of changing of the LC and CNT directors orientations in the magnetic field, according to Fig. 12(a), the PN1–HN transition would occur as a first-order phase transition (see the intersection point of the dotted curves $\Phi = \Psi = 0$ and $\Phi = \pi/2$; $\Psi = 0$) with the jumps in the order parameters of the LC R_n , Q_p and the CNTs R_p , Q_p . The angular phase AN sews the solutions corresponding to the planar phase PN1 and homeotropic phase HN, resulting in the absence of the jumps of the order parameter R_n , Q_p , R_p , and Q_p . Although the curves of the dependencies of these parameters on the magnetic field are continuous, nonmonotone and contain breaking points at $h = h_{\parallel}^{(1)}$ and $h = h_{\perp}$ [see the definitions (20) and (21) as well as Figs. 9(b) and 9(c)].

This is somewhat different in the case of $\xi = 10^4 < \xi_c$, shown in Fig. 12(b). The solutions corresponding to the fixed angles, namely, $\Phi = \Psi = \pi/2$ and $\Phi = \pi/2$; $\Psi = 0$ have the same free-energy densities and differ only by the sign of the order parameter Q_p . Thus, for the second planar phase PN2 at $\Phi = \Psi = \pi/2$ the orientations of the LC and CNT directors are set by the vectors \mathbf{n} and \mathbf{m} , respectively, and the parameter $Q_p > 0$. If we solve the system of orientational state equations for the planar phase PN2 at fixed angles $\Phi = \pi/2$; $\Psi = 0$, the orientations of the LC and CNT directors are determined by the vectors \mathbf{n} and \mathbf{p} (see Fig. 2), respectively, and the parameter $Q_p < 0$. Similarly, for the homeotropic phase HN at $\Phi = \Psi = \pi/2$ the parameter $Q_p < 0$ and the LC and CNT directors are the vectors \mathbf{n} and \mathbf{p} . At $\Phi = \pi/2$, $\Psi = 0$ we obtain $Q_p > 0$ and the LC and CNT directors correspond to the vectors \mathbf{n} and \mathbf{m} . For the range of magnetic fields $h_{\parallel}^{(2)} < h < h_{\perp}$, corresponding to the angular phase AN at any of the above fixed angles options with the growth of the field there is a change in the parameter Q_p sign, which corresponds to the reorientation of the CNTs in the direction of the field [see the dotted lines in Fig. 12(b)]. Figure 12(b) shows that

for $h_{\parallel}^{(2)} < h < h_{\perp}$ the solutions corresponding to the angular phase AN have smaller values of the free-energy density and are therefore thermodynamically stable relative to the solutions that were constructed at fixed angles Φ and $\Psi = 0$. Here, it should be recalled that the angular phase cannot exist at any value of ξ and ω . According to the diagrams shown in Figs. 4–6 there is a triple T point to the left of which there is a direct transition PN2–HN with a change in the Q_p parameter sign without rotations of the CNT and LC directors.

Thus, we can conclude that the direct transition to the homeotropic phase HN occurs from a state in which the LC director is already oriented orthogonal to the magnetic field, i.e., from the second planar phase PN2. The transition to the homeotropic phase HN from the first planar phase PN1 must be accompanied by a rotation of the LC director, i.e., such a transition cannot be direct. It is expected that as the concentration of the impurity y_p increases the situation can be reversed.

-
- [1] I. W. Stewart, *The Static and Dynamic Continuum Theory of Liquid Crystals: A Mathematical Introduction* (Taylor and Francis, Oxford, UK, 2004).
- [2] N. Podoliak, O. Buchnev, O. Buluy, G. D'Alessandro, M. Kaczmarek, Y. Reznikov, and T. J. Sluckin, *Soft Matter* **7**, 4742 (2011).
- [3] A. Mertelj, N. Osterman, D. Lisjak, and M. Čopič, *Soft Matter* **10**, 9065 (2014).
- [4] E. Kadivar and M. Farrokhbin, *Chin. Phys. B* **27**, 046801 (2018).
- [5] Y. Garbovskiy, A. Emelyanenko, and A. Glushchenko, *Nanoscale* **12**, 16438 (2020).
- [6] K. Koch, M. Kundt, A. Eremin, H. Nadası, and A. M. Schmidt, *Phys. Chem. Chem. Phys.* **22**, 2087 (2020).
- [7] K. Koch, M. Kundt, A. Barkane, H. Nadası, S. Webers, J. Landers, H. Wende, A. Eremin, and A. M. Schmidt, *Phys. Chem. Chem. Phys.* **23**, 24557 (2021).
- [8] S. Burylov, D. Petrov, V. Lacková, K. Zakutanská, N. Burylova, A. Voroshilov, V. Skosar, F. Agresti, P. Kopčanský, and N. Tomašovičová, *J. Mol. Liq.* **321**, 114467 (2021).
- [9] M. V. Gorkunov and M. A. Osipov, *Soft Matter* **7**, 4348 (2011).
- [10] L. M. Lopatina and J. V. Selinger, *Phys. Rev. E* **84**, 041703 (2011).
- [11] Y. L. Raikher, V. I. Stepanov, and A. N. Zakhlevnykh, *Soft Matter* **9**, 177 (2013).
- [12] A. Zakhlevnykh, M. Lubnin, and D. Petrov, *J. Magn. Magn. Mater.* **431**, 62 (2017).
- [13] Y. Raikher and V. Stepanov, *J. Mol. Liq.* **267**, 367 (2018).
- [14] D. A. Petrov, A. N. Zakhlevnykh, and A. V. Mantsurov, *J. Exp. Theor. Phys.* **127**, 357 (2018).
- [15] C. Tyszkiewicz, T. Pustelny, and E. Nowinowski-Kruszelnicki, *Eur. Phys. J.: Spec. Top.* **154**, 221 (2008).
- [16] M. Krasna, M. Cvetko, and M. Ambrožič, *Beilstein J. Org. Chem.* **6**, 74 (2010).
- [17] B. Kinkead and T. Hegmann, *J. Mater. Chem.* **20**, 448 (2010).
- [18] N. Tomašovičová, S. Burylov, V. Gdovinová, A. Tarasov, J. Kovac, N. Burylova, A. Voroshilov, P. Kopčanský, and J. Jadzyn, *J. Mol. Liq.* **267**, 390 (2018).
- [19] P. Bury, M. Veveričík, P. Kopčanský, M. Timko, and V. Lacková, *Phys. E* **134**, 114860 (2021).
- [20] A. Cuetos, A. Galindo, and G. Jackson, *Phys. Rev. Lett.* **101**, 237802 (2008).
- [21] S. D. Peroukidis and S. H. L. Klapp, *Phys. Rev. E* **92**, 010501(R) (2015).
- [22] S. D. Peroukidis, K. Lichtner, and S. H. L. Klapp, *Soft Matter* **11**, 5999 (2015).
- [23] M. González-Pinto, Y. Martínez-Ratón, E. Velasco, and S. Varga, *Phys. Chem. Chem. Phys.* **17**, 6389 (2015).
- [24] Q. Liu, P. J. Ackerman, T. C. Lubensky, and I. I. Smalyukh, *Proc. Natl. Acad. Sci. USA* **113**, 10479 (2016).
- [25] S. D. Peroukidis, S. H. L. Klapp, and A. G. Vanakaras, *Soft Matter* **16**, 10667 (2020).
- [26] I. Dierking, G. Scalia, P. Morales, and D. LeClere, *Adv. Mater.* **16**, 865 (2004).
- [27] S. Y. Jeon, K. A. Park, I.-S. Baik, S. J. Jeong, S. H. Jeong, K. H. An, S. H. Lee, and Y. H. Lee, *Nano* **02**, 41 (2007).
- [28] E. Petrescu and C. Cirtoaje, *Beilstein J. Nanotechnol.* **9**, 233 (2018).
- [29] P. Bury, M. Veveričík, P. Kopčanský, M. Timko, and Z. Mitróová, *Phys. E* **103**, 53 (2018).
- [30] R. Basu and D. T. Gess, *Phys. Rev. E* **104**, 054702 (2021).
- [31] A. García-García, R. Vergaz, J. F. Algorri, G. Zito, T. Cacace, A. Marino, J. M. Otón, and M. A. Geday, *Beilstein J. Nanotechnol.* **7**, 825 (2016).
- [32] J.-Y. Lee, L. Bohdan, and K. Jong-Hyun, *Sci. Rep.* **9**, 20223 (2019).
- [33] D. A. Petrov, P. K. Skokov, and A. N. Zakhlevnykh, *Beilstein J. Nanotechnol.* **8**, 2807 (2017).
- [34] D. A. Petrov, P. K. Skokov, A. N. Zakhlevnykh, and D. V. Makarov, *Beilstein J. Nanotechnol.* **10**, 1464 (2019).
- [35] C. Cirtoaje and E. Petrescu, *Materials* **12**, 4031 (2019).
- [36] C. Cirtoaje, G. Iacobescu, and E. Petrescu, *Crystals* **10**, 567 (2020).
- [37] F. Brochard and P. de Gennes, *J. Phys. France* **31**, 691 (1970).
- [38] S. V. Burylov and Y. L. Raikher, *Mol. Cryst. Liq. Cryst. Sci. Technol., Sect. A* **258**, 107 (1995).
- [39] A. Zakhlevnykh, *J. Magn. Magn. Mater.* **269**, 238 (2004).
- [40] S. V. Burylov and A. N. Zakhlevnykh, *Phys. Rev. E* **88**, 052503 (2013).
- [41] D. A. Petrov and A. N. Zakhlevnykh, *J. Mol. Liq.* **287**, 110901 (2019).
- [42] S. Pikin and V. L. Indenbom, *Soviet Physics Uspekhi* **21**, 487 (1978).
- [43] G. R. Luckhurst and T. J. Sluckin, *Biaxial Nematic Liquid Crystals: Theory, Simulation, and Experiment* (John Wiley & Sons, New York, NY, 2015).
- [44] M. V. Gorkunov, M. A. Osipov, A. Kocot, and J. K. Vij, *Phys. Rev. E* **81**, 061702 (2010).
- [45] M. A. Osipov and M. V. Gorkunov, *J. Phys.: Condens. Matter* **22**, 362101 (2010).
- [46] C. Tschierske and D. J. Photinos, *J. Mater. Chem.* **20**, 4263 (2010).
- [47] V. M. Pergamenschchik and V. A. Uzunova, *Phys. Rev. E* **83**, 021701 (2011).
- [48] I. I. Smalyukh, *Rep. Prog. Phys.* **83**, 106601 (2020).

- [49] A. Vats, S. Puri, and V. Banerjee, *Phys. Rev. E* **106**, 044701 (2022).
- [50] A. P. Ramirez, R. C. Haddon, O. Zhou, R. M. Fleming, Z. J., S. M. McClure, and R. E. Smalley, *Science* **265**, 84 (1994).
- [51] M. Fujiwara, E. Oki, M. Hamada, Y. Tanimoto, I. Mukouda, and Y. Shimomura, *J. Phys. Chem. A* **105**, 4383 (2001).
- [52] S. Zaric, G. N. Ostojic, J. Kono, J. Shaver, V. C. Moore, R. H. Hauge, R. E. Smalley, and X. Wei, *Nano Lett.* **4**, 2219 (2004).
- [53] T. A. Searles, Y. Imanaka, T. Takamasu, H. Ajiki, J. A. Fagan, E. K. Hobbie, and J. Kono, *Phys. Rev. Lett.* **105**, 017403 (2010).
- [54] C. Cirtoaje and E. Petrescu, *Phys. E* **84**, 244 (2016).
- [55] P. de Gennes and J. Prost, *The Physics of Liquid Crystals* (Clarendon Press, Oxford, UK, 1993).
- [56] L. Onsager, *Ann. N.Y. Acad. Sci.* **51**, 627 (1949).
- [57] R. F. Kayser and H. J. Raveché, *Phys. Rev. A* **17**, 2067 (1978).
- [58] G. J. Vroege and H. N. W. Lekkerkerker, *Rep. Prog. Phys.* **55**, 1241 (1992).
- [59] L. Mederos, E. Velasco, and Y. Martínez-Ratón, *J. Phys.: Condens. Matter* **26**, 463101 (2014).
- [60] A. N. Zakhlevnykh and M. I. Shliomis, *Zh. Eksp. Teor. Fiz.* **86**, 1309 (1984) [*Sov. Phys. JETP* **59**, 764 (1984)].
- [61] R. Rosso, *Liq. Cryst.* **34**, 737 (2007).
- [62] A. V. Emelyanenko, M. A. Osipov, and D. A. Dunmur, *Phys. Rev. E* **62**, 2340 (2000).
- [63] A. V. Emelyanenko, *Phys. Rev. E* **67**, 031704 (2003).
- [64] S. Rathinavel, K. Priyadharshini, and D. Panda, *Mater. Sci. Eng., B* **268**, 115095 (2021).
- [65] C. Laurent, E. Flahaut, and A. Peigney, *Carbon* **48**, 2994 (2010).
- [66] S. P. Yadav and S. Singh, *Prog. Mater. Sci.* **80**, 38 (2016).
- [67] Z. Mitróová, N. Tomašovičová, M. Timko, M. Koneracká, J. Kováč, J. Jadzyn, I. Vávra, N. Éber, T. Tóth-Katona, E. Beaunon, X. Chaud, and P. Kopčanský, *New J. Chem.* **35**, 1260 (2011).
- [68] O. Buluy, S. Nepijko, V. Reshetnyak, E. Ouskova, V. Zadorozhnii, A. Leonhardt, M. Ritschel, G. Schönhense, and Y. Reznikov, *Soft Matter* **7**, 644 (2011).
- [69] D. Singh, U. B. Singh, M. B. Pandey, R. Dabrowski, and R. Dhar, *Mater. Lett.* **216**, 5 (2018).
- [70] Z. Mitróová, M. Koneracká, N. Tomašovičová, M. Timko, J. Jadzyn, I. Vávra, N. Éber, K. Fodor-Csorba, T. Tóth-Katona, A. Vajda, and P. Kopčanský, *Phys. Procedia* **9**, 41 (2010).
- [71] P. Kaiser, W. Wiese, and S. Hess, *J. Non-Equilib. Thermodyn.* **17**, 153 (1992).
- [72] A. V. Emelyanenko, S. Aya, Y. Sasaki, F. Araoka, K. Ema, K. Ishikawa, and H. Takezoe, *Phys. Rev. E* **84**, 041701 (2011).
- [73] A. V. Emelyanenko, E. S. Filimonova, and A. R. Khokhlov, *Phys. Rev. E* **103**, 022709 (2021).
- [74] D. N. Chausov, A. D. Kurilov, A. I. Smirnova, D. N. Stolbov, R. N. Kucherov, A. V. Emelyanenko, S. V. Saviolov, and N. V. Usol'tseva, *J. Mol. Liq.* **374**, 121139 (2023).